

Organo-Iron Benzaldehyde-Hydrazone Complexes. Synthesis, Characterization, Electrochemical, and Structural Studies[#]

Carolina Manzur,^{*,†} Lorena Millán,[†] Walter Figueroa,[†] Daphne Boys,[‡] Jean-René Hamon,^{*,§} and David Carrillo[†]

Laboratorio de Química Inorgánica, Instituto de Química, Universidad Católica de Valparaíso, Avenida Brasil 2950, Valparaíso, Chile, Departamento de Física, Facultad de Ciencias Físicas y Matemáticas, Universidad de Chile, Casilla 487-3, Santiago, Chile, and UMR 6509 CNRS-Université de Rennes 1, Institut de Chimie de Rennes, Campus de Beaulieu, 35042 Rennes Cedex, France

Received August 19, 2002

A series of new monocationic organo-iron(II) benzaldehyde-hydrazone complexes of general formula $[\text{CpFe}(\eta^6\text{-}o\text{-RC}_6\text{H}_4\text{-NHN=CH-C}_6\text{H}_4\text{-}p\text{-R}')^+] \text{PF}_6^-$ ($\text{Cp} = \eta^5\text{-C}_5\text{H}_5$; $\text{R}, \text{R}' = \text{H}, \text{H}$ **5**; H, Me **6**; H, MeO **7**; H, NMe_2 **8**; Me, Me **9**; Me, MeO **10**; Me, NMe_2 **11**; MeO, Me **12**; MeO, MeO **13**; MeO, NMe_2 **14**; Cl, Me **15**; Cl, MeO **16**; Cl, NMe_2 **17**) have been synthesized. These mononuclear hydrazones were stereoselectively obtained as their *trans*-isomers about the $\text{N}=\text{C}$ double bond, by reaction of the corresponding organometallic hydrazine precursors $[\text{CpFe}(\eta^6\text{-}o\text{-RC}_6\text{H}_4\text{-NHNH}_2)^+] \text{PF}_6^-$ ($\text{R} = \text{H}, \text{1}$; $\text{Me}, \text{2}$; $\text{MeO}, \text{3}$; $\text{Cl}, \text{4}$) with *p*-substituted benzaldehydes $p\text{-R}'\text{C}_6\text{H}_4\text{CHO}$ ($\text{R}' = \text{H}, \text{Me}, \text{MeO}, \text{NMe}_2$) in refluxing ethanol. The *N*-methyl derivatives formulated as $[\text{CpFe}\{\eta^6\text{-C}_6\text{H}_5\text{-N}(\text{Me})\text{N=CH-C}_6\text{H}_4\text{-}p\text{-R}'\}]^+ \text{PF}_6^-$ ($\text{R}' = \text{Me}, \text{18}$; $\text{MeO}, \text{19}$; $\text{NMe}_2, \text{20}$) are readily prepared by deprotonation of complexes **6–8** with *n*-butyllithium and subsequent alkylation with iodomethane in THF at -70°C . All these complexes have been fully characterized by elemental analysis, IR, UV–vis, and ^1H NMR spectroscopies, and mass spectrometry for compounds **10**, **12**, and **16**. Complexes **6** and **19** have also been characterized by single-crystal X-ray diffraction analysis. One of the more salient features of these structures is the long $\text{Fe-C}_{\text{ipso}}$ bond distances and the slight cyclohexadienyl character at the coordinated C_6 ring with a folding angle of 6.2° and 7.4° , respectively. Moreover, the two phenyl rings of each compound are almost coplanar with a dihedral angle of 4.9° for **6** and 6.2° for **19**. Cyclic voltammetry of the benzaldehyde-hydrazone complexes **5–8**, **11**, **14**, and **17** in DMF shows an irreversible reduction wave at ca. -1.92 V vs Ag/AgCl , depending on the nature of both R and $p\text{-R}'$ substituents, corresponding to the reduction of an in situ generated zwitterionic Fe(II) intermediate. The irreversible reduction waves of the cationic *N*-methylated hydrazones **18–20** are observed in the expected range -1.35 to -1.47 V vs Ag/AgCl , either in DMF or in acetonitrile.

Introduction

The design and synthesis of robust electron-acceptor mixed-sandwich derivatives $[\text{CpFe}(\eta^6\text{-arene})]^+$ ($\text{Cp} = \eta^5\text{-C}_5\text{H}_5$) have long been of interest due to their important position in the development of organometallic¹ and metal-assisted organic chemistry,² and more recently as organometallic route to dendrimers using the CpFe^+ induced polyfunctionalization³ of polymethylbenzenes.

Moreover, their interesting redox properties⁴ allow studies of electronic communication between ligand-bridged metals.⁵ Despite these intense investigations, only in one case the $[\text{CpFe}(\eta^6\text{-aryl})]^+$ moiety has been used as organometallic chromophore to achieve second-order nonlinear optical (NLO) responses.⁶ Hydrazones possess an asymmetric transmitter backbone -NHN=CH- that allows the formation of two different types of compounds: A-NHN=CH-D (type I) and D-NHN=CH-A (type II), where A and D are, respectively, acceptor and donor entities.⁷ Thus, we reasoned that

[#] This article is dedicated to Professor Pierre Gouzerh, a distinguished friend and colleague, on the occasion of his 60th birthday.

^{*} To whom correspondence should be addressed. E-mail: jean-rene.hamon@univ-rennes1.fr.

[†] Universidad Católica de Valparaíso, Chile.

[‡] Universidad de Chile.

[§] Université de Rennes 1, France.

(1) (a) Abd-El-Aziz, A. S.; Bernardin, S. *Coord. Chem. Rev.* **2000**, *203*, 219. (b) Astruc, D. *The Chemistry of the Metal-Carbon Bond*; Hartley F. R., Patai, S., Eds.; Wiley: New York, 1987; Vol. 4, p 625. (c) Sutherland, R. G.; Igbal, M.; Piorkó, A. *J. Organomet. Chem.* **1986**, *302*, 307. (d) Sutherland, R. G. *J. Organomet. Chem. Libr.* **1977**, *3*, 311.

(2) (a) Astruc, D. *Tetrahedron* **1983**, *39*, 4027. (b) Astruc, D. *Top. Curr. Chem.* **1991**, *160*, 47.

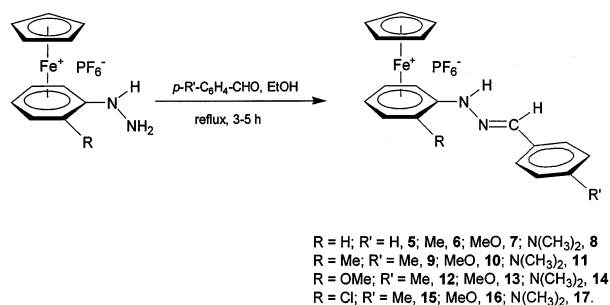
(3) (a) Astruc, D.; Blais, J.-C.; Cloutet, E. Djakovitch, L.; Rigaut, S.; Ruiz, J.; Sartor, V.; Valério, C. In *Dendrimers II; Architecture, Nanostructure and Supramolecular Chemistry*; Vögtle, F., Ed.; *Topics in Current Chemistry*; Springer-Verlag: Berlin, 2000; Vol. 120, p 229. (b) Nlate, S.; Nieto, Y.; Blais, J.-C.; Ruiz, J.; Astruc, D. *Chem. Eur. J.* **2002**, *8*, 171. (c) Alonso, B.; Blais, J.-C.; Astruc, D. *Organometallics* **2002**, *21*, 1001.

(4) Astruc, D. *Chem. Rev.* **1988**, *88*, 1189.

(5) Astruc, D. *Acc. Chem. Res.* **1997**, *30*, 383.

(6) Lambert, C.; Gaschler, W.; Zabel, M.; Matschiner, R.; Wortmann, R. *J. Organomet. Chem.* **1999**, *592*, 109.

Scheme 1



complexation of one aromatic ring of a free organic hydrazone with the 12-electron cationic organometallic moiety [CpFe]⁺ will lead to the acceptor fragment [CpFe(η^6 -arylhydrazone)]⁺, and along this line, we have successfully prepared new Type I organometallic architectures.⁸

As a part of our ongoing research program on the chemistry of organo-iron hydrazones, in this contribution we report: (i) the synthesis and full spectroscopic characterization of a series of thirteen new organo-iron(II) benzaldehyde-hydrazone complexes of the general form [CpFe(η^6 -*o*-RC₆H₄-NHN=CH-C₆H₄-*p*-R')]PF₆⁻ (**5–17**) that contain a R group as *ortho*-substituent of the coordinated phenyl ring (R = H, Me, MeO, Cl) and a R' donor-substituent groups (R' = Me, MeO, NMe₂) at the *para*-positions of the free arene (see Scheme 1), and of three derivatized *N*-methyl benzaldehyde-hydrazone complexes of general formula [CpFe(η^6 -C₆H₅-N(Me)N=CH-C₆H₄-*p*-R')]PF₆⁻ (**18–20**; see Scheme 2); (ii) the X-ray crystal structures of a representative example of each series, namely compounds **6** (R, R' = H, Me) and **19** (R' = MeO), and (iii) the electrochemical behavior of three selected classes of these organometallic hydrazones in both acetonitrile and DMF.

Experimental Section

General Data. All operations were performed under inert atmosphere using standard vacuum/nitrogen line, Schlenk or syringe techniques with protection of light. Solvents were dried and distilled under nitrogen by standard methods prior to use. Microanalytical data were obtained on a Perkin-Elmer Model 2400 elemental analyzer, and by the Centre for Microanalyses of the CNRS at Vernaison (France). IR spectra were obtained with a Perkin-Elmer Model 1600 FT-IR spectrophotometer. Electronic spectra were recorded in CH₂Cl₂ and DMSO solutions with a Spectronic Genesys 2 spectrophotometer. All the ¹H NMR spectra were recorded in

acetone-*d*₆ on a multinuclear Bruker DPX 200 spectrometer (200 MHz) at 297 K, and all chemical shifts are reported in parts per million (ppm) relative to internal tetramethylsilane (Me₄Si), with the residual solvent proton resonance as internal standards. Coupling constants are given in Hertz (Hz). Mass spectra were recorded at the Centre Régional de Mesures Physiques de l'Ouest (C. R. M. P. O.) Rennes, in a high-resolution ZabSpec TOF VG Analytical spectrometer operating in the LSIMS⁺ mode. Ions were produced with the standard Cs⁺ gun at ca. 8 kV, poly(ethylene glycol) (PEG) was used as internal reference and 3-nitrobenzyl alcohol (NBA) was used as the matrix. All mass measurements refer to peaks for the most common isotopes (¹H, ¹²C, ¹⁴N, ¹⁶O, ³⁵Cl, ⁵⁶Fe). Electrochemical measurements were performed using a Radiometer Analytical model PGZ 100 All-in-one potentiostat, using a standard three-electrode setup with a vitreous carbon working and platinum wire auxiliary electrodes and a Ag/AgCl as the reference electrode. DMF and acetonitrile solutions were 1.0 mM in the compound under study and 0.1 M in the supporting electrolyte *n*-Bu₄N⁺PF₆⁻. Melting points were determined in evacuated capillaries and were not corrected. Reagents were obtained as follows: benzaldehyde and its *p*-substituted derivatives 4-methyl-, 4-methoxy and 4-*N,N*-dimethyl-benzaldehyde, *n*-butyllithium 1.6 M in hexane, iodomethane, were purchased from commercial sources and used as received. The hydrazine complexes [CpFe(η^6 -C₆H₅NHNH₂)]⁺PF₆⁻ (**1**) and [CpFe(η^6 -*o*-ClC₆H₄NHNH₂)]⁺PF₆⁻ (**4**) were synthesized according to literature methods,⁹ starting from [CpFe(η^6 -C₆H₅Cl)]⁺PF₆⁻¹⁰ and [CpFe(η^6 -*o*-Cl₂C₆H₄)]⁺PF₆⁻¹¹ Likewise, the hydrazine complexes [CpFe(η^6 -*o*-MeC₆H₄NHNH₂)]⁺PF₆⁻ (**2**) and [CpFe(η^6 -*o*-MeOC₆H₄NHNH₂)]⁺PF₆⁻ (**3**) were prepared according to our previously published procedures.¹²

Preparation of the Hydrazones Complexes 5–17.

General Procedure. A mixture of the indicated quantities of the solid [CpFe(η^6 -*o*-RC₆H₄NHNH₂)]⁺PF₆⁻ (R = H, **1**; Me, **2**; MeO, **3**; Cl, **4**) and benzaldehyde *p*-R'₆H₄CHO (R' = H, Me, MeO, NMe₂) was treated in 5 mL ethanol containing 5 drops of concentrated acetic acid. The solution was refluxed for 3–5 h, allowed to stand at room temperature and then at -25 °C overnight (12 h). The precipitate was filtered off, washed with 5 mL of diethyl ether and dried under vacuum. Recrystallization from dichloromethane or acetonitrile by slow diffusion of diethyl ether at room temperature provided the products as crystalline solids (see Supporting Information, Table S1, for reagents, stoichiometries and yields).

Scheme 2

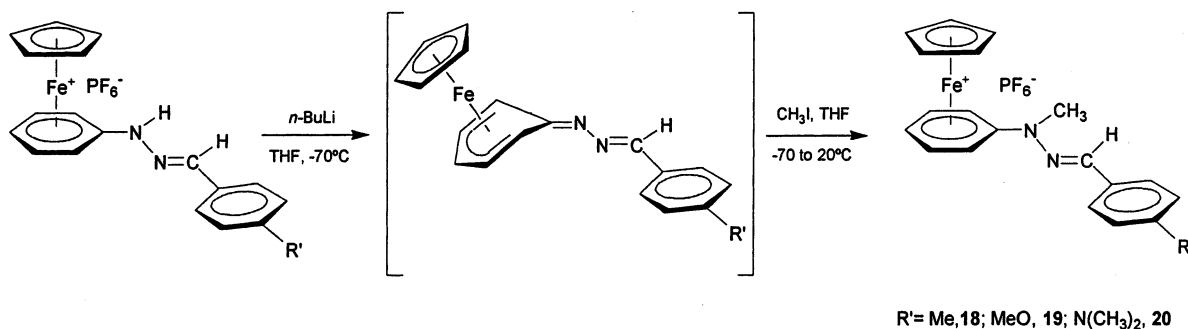


Table 1. Spectroscopic Data of the New Iron Hydrazone Complexes

compound	IR (KBr, ν/cm^{-1})	UV-vis (λ/nm , $\log \epsilon/\text{L mol}^{-1} \text{cm}^{-1}$)	$^1\text{H NMR}$ (δ/ppm , acetone- d_6)
5	3334w (NH), 1567s (C=N), 843vs and 558s (PF ₆)	(CH ₂ Cl ₂): 243 (4.21), 292 (4.10) (sh), 319 (4.18), 340 (4.12) (sh), 413 (3.10) (DMSO ^a): 292 (4.04) (sh), 317 (4.17) (sh), 343 (4.23), 406 (3.29)	5.15 (s, 5H, Cp ^a), 6.26 (t, 1H, coord-Ph ^a , $J_{\text{HH}} = 5.8$), 6.42 (<i>pseudo</i> -t, 2H, coord-Ph), 6.52–6.56 (m, 2 H, coord-Ph), 7.52–7.56 (m, 3H, Ph), 7.87–7.92 (m, 2H, Ph), 8.21 (s, 1H, =CH), 9.89 (s, 1H, NH)
6	3331m (NH), 1567s (C=N), 832vs and 558s (PF ₆)	(CH ₂ Cl ₂): 244 (4.19), 297 (4.09) (sh), 321 (4.17), 340 (4.10) (sh), 411 (3.19) (DMSO): 294 (4.18) (sh), 322 (4.32) (sh), 344 (4.36), 408 (3.45)	2.45 (s, 3H, Me ^a), 5.13 (s, 5H, Cp), 6.28 (t, 1H, coord-Ph, $J_{\text{HH}} = 5.8$), 6.41 (<i>pseudo</i> -t, 2H, coord-Ph), 6.52 (d, 2H, coord-Ph, $J_{\text{HH}} = 6.6$), 7.37 (d, 2H, Ph, $J_{\text{HH}} = 7.9$), 7.78 (d, 2H, Ph, $J_{\text{HH}} = 8.0$), 8.16 (s, 1H, =CH), 9.80 (s, 1H, NH)
7	3337m (NH), 1564s (C=N), 1250s (OMe), 844vs and 558s (PF ₆)	(CH ₂ Cl ₂): 248 (4.26), 304 (4.21) (sh), 327 (4.31), 340 (4.28) (sh), 412 (3.39) (DMSO): 291 (3.98) (sh), 329 (4.13) (sh), 348 (4.16), 399 (3.28)	3.94(s, 3H, OMe), 5.13 (s, 5H, Cp), 6.24 (m, 1H, coord-Ph), 6.40 (<i>pseudo</i> -t, 2H, coord-Ph), 6.49 (t, 2H, coord-Ph, $J_{\text{HH}} = 6.6$), 7.11 (d, 2H, Ph, $J_{\text{HH}} = 8.8$), 7.84 (d, 2H, Ph, $J_{\text{HH}} = 8.8$), 8.15 (s, 1H, =CH), 9.81 (s, 1H, NH)
8	3320m (NH), 1560s (C=N), 832vs and 558s (PF ₆)	(CH ₂ Cl ₂): 243 (4.20), 265 (4.03) (sh), 324 (4.14) (sh), 367 (4.36), 433 (3.73) (DMSO): 330 (3.56) (sh), 371 (3.84), 428 (3.13)	3.11 (s, 6H, NMe ₂), 5.11 (s, 5H, Cp), 6.22 (t, 1H, coord-Ph, $J_{\text{HH}} = 5.6$), 6.33–6.44 (m, 4H, coord-Ph), 6.78 (d, 2H, Ph, $J_{\text{HH}} = 8.9$), 7.71 (d, 2H, Ph, $J_{\text{HH}} = 8.9$), 8.07 (s, 1H, =CH), 9.60 (s, 1H, NH)
9	3384m (NH), 1555s (C=N), 847vs and 559s (PF ₆)	(CH ₂ Cl ₂): 245 (4.32), 292 (4.20), 309 (4.33), 411 (3.15) (DMSO): 289 (4.07) (sh), 326 (4.18), 342 (4.11) (sh), 406(3.23)	2.55 (s, 3H, Me), 2.66 (s, 3H, Me), 5.11 (s, 5H, Cp), 6.12 (t, 1H, coord-Ph, $J_{\text{HH}} = 6.0$), 6.31–6.33 (m, 2H, coord-Ph), 6.86 (d, 1H, coord-Ph, $J_{\text{HH}} = 6.5$), 7.44 (d, 2H, Ph, $J_{\text{HH}} = 8.0$), 7.96 (d, 2H, Ph, $J_{\text{HH}} = 8.0$), 8.12 (s, 1H, =CH), 8.91 (s, 1H, NH)
10^b	3347w (NH), 1558m (C=N), 1250m (OMe), 842vs and 558s (PF ₆)	(CH ₂ Cl ₂): 247 (4.28), 291 (4.17) (sh), 326 (4.33), 340 (4.29) (sh), 413 (3.34) (DMSO): 291 (4.23) (sh), 330 (4.40) (sh), 344 (4.42), 407 (3.52)	2.63(s, 3H, Me), 3.94 (s, 3H, OMe), 5.06 (s, 5H, Cp), 6.11–6.37 (m, 3H, coord-Ph), 6.89 (d, 1H, coord-Ph, $J_{\text{HH}} = 6.6$), 7.11 (d, 2H, Ph, $J_{\text{HH}} = 8.8$), 7.84 (d, 2H, Ph, $J_{\text{HH}} = 8.8$), 8.32 (s, 1H, =CH), 9.32 (s, 1H, NH)
11	3343m (NH), 1528s (C=N), 842vs, 830vs and 558s (PF ₆)	(CH ₂ Cl ₂): 244 (4.28), 267 (4.03) (sh), 320 (4.15) (sh), 368 (4.41), 429 (3.78) (DMSO): 321 (3.29) (sh), 371 (3.60), 429 (2.87)	2.61 (s, 3H, Me), 3.11 (s, 6H, NMe ₂), 5.04 (s, 5H, Cp), 6.12 (t, 1H, coord-Ph, $J_{\text{HH}} = 6.0$), 6.29–6.35 (m, 2H, coord-Ph), 6.83 (d, 1H, coord-Ph, $J_{\text{HH}} = 7.1$), 6.88 (d, 2H, Ph, $J_{\text{HH}} = 8.6$), 7.72 (d, 2 H, Ph, $J_{\text{HH}} = 8.9$), 8.24 (s, 1H, =CH), 9.18 (s, 1H, NH)
12^c	3333m (NH), 1558s (C=N), 1275s (OMe), 841vs and 557s (PF ₆)	(CH ₂ Cl ₂): 244 (4.36), 288 (4.11) (sh), 325 (4.31), 341 (4.28) (sh), 419 (3.25) (DMSO): 293 (3.61) (sh), 327 (3.84) (sh), 347 (3.88), 416 (2.89)	2.45 (s, 3H, Me), 4.24 (s, 3H, OMe), 5.06 (s, 5H, Cp), 6.04–6.16 (m, 2H, coord-Ph), 6.53 (d, 1H, coord-Ph, $J_{\text{HH}} = 6.2$), 6.92 (d, 1H, coord-Ph, $J_{\text{HH}} = 6.4$), 7.37 (d, 2H, Ph, $J_{\text{HH}} = 7.9$), 7.79 (d, 2H, Ph, $J_{\text{HH}} = 8.1$), 8.39 (s, 1H, =CH), 9.58 (s, 1H, NH)
13	3345m (NH), 1564s (C=N), 1250s (OMe), 844vs and 558s (PF ₆)	(CH ₂ Cl ₂): 248 (4.37), 291 (4.24) (sh), 322 (4.32), 419 (3.33) (DMSO): 287 (4.28) (sh), 326 (4.39), 346 (4.32) (sh), 417 (3.40)	3.90 (s, 3H, OMe), 4.10 (s, 3H, OMe), 5.06 (s, 5H, Cp), 6.64–6.97 (m, 4H, coord-Ph), 7.11 (d, 2H, Ph, $J_{\text{HH}} = 8.8$), 7.84 (d, 2H, Ph, $J_{\text{HH}} = 8.8$), 8.32 (s, 1H, =CH), 9.35 (s, 1H, NH)
14	3328m (NH), 1564m (C=N), 1273m (OMe), 842vs and 559s (PF ₆)	(CH ₂ Cl ₂): 241 (4.31), 264 (4.11) (sh), 320 (4.17) (sh), 372 (4.48), 437 (3.82) (DMSO): 310 (3.93) (sh), 371 (4.26), 437 (3.60)	3.12 (s, 6H, NMe ₂), 4.24 (s, 3H, OMe), 5.05 (s, 5H, Cp), 6.04–6.12 (m, 2H, coord-Ph), 6.50 (d, 1H, coord-Ph, $J_{\text{HH}} = 6.2$), 6.86 (<i>pseudo</i> -t, 3H, coord-Ph and Ph), 7.76 (d, 2H, Ph, $J_{\text{HH}} = 9.1$), 8.30 (s, 1H, =CH), 9.30 (s, 1H, NH)
15	3328m (NH), 1560s (C=N), 1049m (C-Cl), 847vs, 829vs and 559s (PF ₆)	(CH ₂ Cl ₂): 247 (4.41), 300 (4.30) (sh), 318 (4.37), 340 (4.30) (sh), 411 (3.34) (DMSO): 296 (3.94) (sh), 327 (4.09), 400 (3.18)	2.47 (s, 3H, Me), 5.21 (s, 5H, Cp), 6.38 (t, 1 H, coord-Ph, $J_{\text{HH}} = 6.0$), 6.46 (t, 1H, coord-Ph, $J_{\text{HH}} = 6.0$), 6.82 (d, 1H, coord-Ph, $J_{\text{HH}} = 6.2$), 7.13 (d, 1H, coord-Ph, $J_{\text{HH}} = 6.6$), 7.39 (d, 2 H, Ph, $J_{\text{HH}} = 7.9$), 7.82 (d, 2H, Ph, $J_{\text{HH}} = 8.1$), 8.47 (s, 1H, =CH), 9.76 (s, 1H, NH)
16^d	3322w (NH), 1560s (C=N), 1255m (OMe), 1169w (C-Cl), 841vs and 558s (PF ₆)	(CH ₂ Cl ₂): 250 (4.27), 302 (4.20) (sh), 326 (4.32), 344 (4.26) (sh), 411 (3.40) (DMSO): 291 (4.19) (sh), 321 (4.24), 348 (4.15) (sh), 402 (3.34)	3.96 (s, 3H, OMe), 5.20 (s, 5H, Cp), 6.33 (<i>pseudo</i> -t, 1H, coord-Ph), 6.45 (<i>pseudo</i> -t, 1H, coord-Ph), 6.81 (d, 1H, coord-Ph, $J_{\text{HH}} = 5.9$), 7.10 (<i>pseudo</i> -t, 3H, coord-Ph and Ph), 7.87 (d, 2H, Ph, $J_{\text{HH}} = 8.9$), 8.46 (s, 1H, =CH), 9.68 (s, 1H, NH)

Table 1 (Continued)

compound	IR (KBr, ν/cm^{-1})	UV-vis (λ/nm , $\log \epsilon/\text{L mol}^{-1} \text{cm}^{-1}$)	$^1\text{H NMR}$ (δ/ppm , acetone- d_6)
17	3318w (NH), 1560s (C=N), 1181s (C-Cl), 844vs, 833vs and 558s (PF ₆)	(CH ₂ Cl ₂): 245 (4.31), 270 (4.07) (sh), 320 (4.16) (sh), 367 (4.45), 435 (3.87) (DMSO): 330 (4.06) (sh), 369 (4.26), 434 (3.61)	3.15 (br s, 6H, NMe ₂), 5.19 (s, 5H, Cp), 6.31 (t, 1H, coord-Ph, $J_{\text{HH}} = 6.2$), 6.43 (t, 1H, coord-Ph, $J_{\text{HH}} = 6.2$), 6.78 (d, 1H, coord-Ph, $J_{\text{HH}} = 6.9$), 6.93 (br d, 2H, Ph, $J_{\text{HH}} = 8.4$), 7.03 (d, 1H, coord-Ph, $J_{\text{HH}} = 6.7$), 7.76 (d, 2H, Ph, $J_{\text{HH}} = 8.6$), 8.37 (s, 1H, =CH), 9.54 (s, 1H, NH)
18	1538s (C=N), 840vs and 558s (PF ₆)	(CH ₂ Cl ₂): 245 (4.24), 298 (4.04) (sh), 328 (4.14), 406 (3.25) (DMSO): 288 (3.73) (sh), 326 (3.94) (sh), 343 (3.97), 409 (3.09)	2.46 (s, 3H, Me), 3.74 (s, 3H, NMe), 5.20 (s, 5H, Cp), 6.36 (t, 1H, coord-Ph, $J_{\text{HH}} = 5.8$), 6.50 (<i>pseudo</i> -t, 2H, coord-Ph), 6.88 (d, 2H, coord-Ph, $J_{\text{HH}} = 6.7$), 7.38 (d, 2H, Ph, $J_{\text{HH}} = 8.0$), 7.86 (d, 2H, Ph, $J_{\text{HH}} = 8.0$), 8.19 (s, 1H, =CH)
19	1542s (C=N), 1249s (OMe), 842vs and 557s (PF ₆)	(CH ₂ Cl ₂): 250 (3.40), 300 (3.50) (sh), 303 (3.48) (sh), 333 (3.52), 413 (3.62) (DMSO): 292 (3.43) (sh), 332 (2.10) (sh), 345 (3.54), 412 (3.62)	3.62 (s, 3H, OMe), 3.87 (s, 3H, NMe), 5.08 (s, 5H, Cp), 6.21 (t, 1H, coord-Ph, $J_{\text{HH}} = 5.8$), 6.36 (<i>pseudo</i> -t, 2H, coord-Ph), 6.72 (d, 2H, coord-Ph, $J_{\text{HH}} = 6.9$), 7.03 (d, 2H, Ph, $J_{\text{HH}} = 8.6$), 7.84 (d, 2H, Ph, $J_{\text{HH}} = 8.9$), 8.09 (s, 1H, =CH)
20	1540s (C=N), 840vs and 558s (PF ₆)	(CH ₂ Cl ₂): 243 (4.11), 269 (3.86) (sh), 320 (4.00) (sh), 367 (4.21), 434 (3.57) (DMSO): 267 (3.99) (sh), 323 (4.12), 369 (4.33), 426 (3.70)	3.12 (s, 6H, NMe ₂), 3.69 (s, 3H, NMe), 5.16 (s, 5H, Cp), 6.28 (t, 1H, coord-Ph, $J_{\text{HH}} = 5.8$), 6.43 (<i>pseudo</i> -t, 2H, coord-Ph), 6.76 (d, 2H, coord-Ph, $J_{\text{HH}} = 6.9$), 6.89 (d, 2H, Ph, $J_{\text{HH}} = 8.9$), 7.80 (d, 2H, Ph, $J_{\text{HH}} = 8.9$), 8.12 (s, 1H, =CH)

^a Abbreviations: Me = CH₃, Cp = C₅H₅, Ph = C₆H₄, DMSO = (CH₃)₂SO. ^b HRMS: $m/z = 361.1003$ (C⁺, 100%), m/z expected for C₂₀H₂₁FeN₂O, 361.1003. ^c HRMS: $m/z = 361.1005$ (C⁺, 100%), m/z expected for C₂₀H₂₁FeN₂O, 361.1003. ^d HRMS: $m/z = 381.0458$ (C⁺, 100%), m/z expected for C₁₉H₁₈ClFeN₂O, 381.0457.

Preparation of the *N*-Methylated Hydrazone Complexes 18–20. General Procedure. To a suspension of indicated quantities of solid hydrazone complex **6–8** (0.15 mmol) in 5 mL of dry THF at -70°C , were slowly added by syringe 94 μL (0.15 mmol) of *n*-BuLi. A deep red color developed immediately. The mixture was stirred for 5 min, and then 93 μL (0.15 mmol) of iodomethane were introduced by syringe. The stirring was continued and the reaction mixture allowed to slowly warm to room temperature, while the color changed gradually to orange. The volatils were removed under vacuum and the solid residue was dissolved in 3 mL of acetonitrile. The solution was filtered and after the addition of 3 mL of diethyl ether, the reaction mixture was stored at -30°C overnight (12 h). The precipitate was filtered off, dissolved in 2 mL of dichloromethane and filtered through Celite. The filtrate was concentrated to half of its volume, and crystallization from dichloromethane diethyl ether mixture gave the products as crystalline solids (see Supporting Information, Table S2, for reagents, stoichiometries and yields).

Analytical and melting point data of the new compounds **5–20** so prepared are given as Supporting

Information (see Table S3). IR, UV-vis, and $^1\text{H NMR}$ data are gathered in Table 1.

X-ray Crystallography. Structure Determination of 6 and 19. Single crystals of [CpFe(η^6 -C₆H₅-NHN=CH-C₆H₄-*p*-Me)]⁺PF₆⁻ (**6**) and of [CpFe(η^6 -C₆H₅-N(Me)N=CH-C₆H₄-*p*-OMe)]⁺PF₆⁻ (**19**) were obtained by slow diffusion of diethyl ether into solutions of **6** and **19** in dichloromethane. A summary of the crystallographic data is given in Table 2. Complete details of the crystal data, X-ray data collection, and structure solution are provided as Supporting Information. Semiempirical corrections, via psi scans were applied for absorption. Cell parameters were obtained from least-squares fit of 58 reflections with $8^\circ \leq 2\theta \leq 30^\circ$. The structures were solved by Patterson and subsequent difference Fourier synthesis. All non-H atoms were refined anisotropically by full-matrix least-squares on all F^2 data with SHELXL-97.¹³ A riding model was adopted for H atoms which were placed at idealized positions with isotropic thermal displacement parameters equal to 1.2 times the equivalent isotropic U_{eq} value of their attached atoms. Displacement parameters highly anisotropic were noted for the C atoms of the C₅H₅ ligand of complex **19**; however, further attempts with disordered positions did not converge.

Results and Discussion

1. Synthesis and Spectroscopy. The syntheses of the mononuclear benzaldehyde-hydrazones **5–17** (see the Experimental Section) were successfully accomplished by reaction of the organometallic hydrazine precursors [CpFe(η^6 -*o*-RC₆H₄NHNH₂)]⁺PF₆⁻ (R = H, **1**;

(13) Sheldrick, G. M. *SHELXL-97, Program for the Refinement of Crystal Structures*; University of Göttingen: Göttingen, Germany, 1997.

(7) (a) Serbutoviez, C.; Bosshard, C.; Knöpfle, G.; Weiss, P.; Prêtre, P.; Günter, P.; Schenk, K.; Solari, E.; Chapuis, G. *Chem. Mater.* **1995**, *7*, 1198. (b) Wong, M. S.; Meier, U.; Pan, F.; Gramlich, V.; Bosshard, C.; Günter, P. *Adv. Mater.* **1996**, *8*, 416. (c) Liakatas, I.; Wong, M. S.; Gramlich, V.; Bosshard, C.; Günter, P. *Adv. Mater.* **1998**, *10*, 777.

(8) Manzur, C.; Millán, L.; Fuentealba, M.; Hamon, J.-R.; Carrillo, D. *Tetrahedron Lett.* **2000**, *41*, 3615.

(9) (a) Neto, A. F.; Miller, J. *An. Acad. Brasil. Cienc.* **1982**, *54*, 331. (b) Lee, C. C.; Abd-El-Aziz, A. S.; Chowdhury, R. L.; Gill, U. S.; Piórko, A.; Sutherland, R. G. *J. Organomet. Chem.* **1986**, *315*, 79.

(10) Nesmeyanov, A. N.; Vol'kenau, N. A.; Bolesova, I. S. *Dokl. Akad. Nauk, SSSR* **1966**, *166*, 607.

(11) Khand, I. U.; Pauson, P. L.; Watts, W. E. *J. Chem. Soc. C* **1968**, 2261.

(12) Manzur, C.; Baeza, E.; Millán, L.; Fuentealba, M.; Hamon, P.; Hamon, J.-R.; Boys, D.; Carrillo, D. *J. Organomet. Chem.*, **2000**, *608*, 126.

Table 2. Crystal Data and Structure Refinement for Complexes 6 and 19

	6	19
empirical formula	C ₁₉ H ₁₉ F ₆ FeN ₂ P	C ₂₀ H ₂₁ F ₆ FeN ₂ OP
formula mass, g mol ⁻¹	476.18	506.21
collection T, K	293(2)	293(2)
cryst syst	tetragonal	monoclinic
space group	P4 ₂ /n	P2 ₁ /c
a (Å)	19.445(2)	6.818(1)
b (Å)	19.445(2)	17.663(4)
c (Å)	10.489(3)	17.828(3)
α, β, γ (deg)	90, 90, 90	90, 98.26(2), 90
V (Å ³)	3966.0(13)	2124.7(7)
Z	8	4
D _{calcd} (g cm ⁻³)	1.595	1.582
cryst size (mm)	0.50 × 0.50 × 0.50	0.40 × 0.10 × 0.08
F(000)	1936	1032
abs coeff (cm ⁻¹)	9.03	8.52
θ range (deg)	2.09–27.56	1.63–25.05
diffractometer	Siemens R3m/V	Siemens R3m/V
αλ(Mo Kα) (Å)	0.71073	0.71073
range h, k, l	–25/0, 0/25, 0/13	–4/8, 0/21, –21/21
no. total reflns	4804	4351
no. unique reflns	4544	3768
no. obsd reflns [<i>I</i> > 2σ(<i>I</i>)]	2666	1295
no. of restraints/params	0/262	0/335
final R	0.0465	0.0504
wR2	0.1234	0.0614
R indices (all data)	0.0848	0.1793
wR2 (all data)	0.1373	0.0769
goodness of fit/F ²	0.947	0.800

Me, **2**; MeO, **3**; Cl, **4**) with benzaldehydes in ethanol containing concentrated acetic acid (Scheme 1). Reaction between **1** and C₆H₅CHO provides the parent complex **5**, whereas reactions of the corresponding *p*-substituted benzaldehyde derivatives *p*-R'C₆H₄CHO (R' = Me, MeO, NMe₂) lead to the formation of compounds **6–17**.

The organometallic hydrazones **5–17** were obtained as air stable orange microcrystalline solids in yields ranging from 59 to 97% (see Table S1). They exhibit high solubility in CH₂Cl₂, MeCN, Me₂CO, and DMSO and are fairly light-sensitive in solution. The structures of these new hydrazones were inferred from satisfactory elemental analyses, ¹H NMR, IR, and UV–vis spectroscopies (see Table 1), and an X-ray diffraction study of **6** (*vide infra*). On the other hand, the LSIMS⁺ mass spectra of compounds **10**, **12**, and **16** exhibit molecular ions (100%) corresponding to the cationic fragment C⁺ with the characteristic isotopic distribution patterns. The most outstanding feature observed in the IR spectra of these 13 powdered compounds **5–17** (see Table 1) was the existence of a sharp intense band in the range 1528–1567 cm⁻¹, which is due to the asymmetric stretching of the C=N imine group. In addition, the infrared spectra showed the typical weak to medium stretching band of the N–H fragment¹⁴ in the region from 3318 to 3384 cm⁻¹, a very strong ν(PF₆) band in the range 829–847 cm⁻¹, which, in some cases, is observed as two well-resolved absorption bands, and a sharp and strong δ(P–F) band at 557–559 cm⁻¹. There are additional weaker bands in the range 1550–1650 cm⁻¹, which occurred for all the complexes and cannot be unequivocally assigned. These vibrations could indeed be attributed to either a carbon–nitrogen stretching fre-

quency of the arene *N* system (see Section 2 below) or carbon–carbon stretching frequencies.¹⁵

Interestingly, the mononuclear organometallic hydrazones **5–17** are stereoselectively formed as a single isomer (about the N=C double bond), as demonstrated by the unique C₅-ring proton resonance in the 5.04–5.21 ppm region for each compound in their respective ¹H NMR spectra (acetone-*d*₆, 297 K, see Table 1). The sterically less hindered *trans*-isomer can be confidently attributed on the basis of previous detailed NMR studies on related binuclear systems¹⁶ and on the crystal structure of compound **6** (see below). The ¹H NMR spectra show also the following general features: (i) a broad signal in the 8.91–9.89 ppm range attributed to the NH proton resonance which is observed at low field due to the electron-withdrawing properties of the [CpFe]⁺ cationic moiety linked to the phenyl ring, (ii) a sharp proton resonance in the 8.07–8.47 ppm region, assigned to the azomethine fragment, N=CH, and (iii) an upfield shift (δ < 7.2) of the aromatic protons of the coordinated C₆-ring relative to those of the free arene.

Benzylic C–H bond activation in cationic arene-cyclopentadienyliron complexes and subsequent bond formation of the resulting neutral cyclohexadienyl species with various elements is a well-established general and useful procedure for effecting modifications on the structure of the arene ligand.^{2b,3,17} It is made possible by the enhancement of the acidity of the benzylic protons in the cationic complex. For instance, the p*K*_a in DMSO has indeed been found to be about 14 units lower for the 18-electron complexes [CpM(η⁶-C₆Me₆)]⁺PF₆⁻ (M = Fe, Ru; p*K*_a = 29) than for the free arene (p*K*_a = 43).^{18–20} On the other hand, several authors^{15a,21–23} have also demonstrated that deprotonation could occur at the amino substituent on the arene ligand and that subsequent treatment with an excess of alkylating reagents give rise to formation of new N–C bonds. Accordingly, the *N*-Me hydrazone derivatives **18–20** were obtained from their respective *N*-H hydrazone precursors **6–8** in a one-pot two-step sequence (see the Experimental Section and Table S2). The red zwitterionic intermediate is first generated at low temperature in dry tetrahydrofuran (THF) by deprotonating the benzylic –NH– group with *n*-butyllithium and then quenched with iodomethane to provide the final *N*-methylated hydrazones (Scheme 2).

The three new *N*-methylated benzaldehyde-hydrazone complexes **18–20** were isolated as air and thermally stable orange-red crystalline solids in yields ranging from 53 to 66%. Their elemental analyses are consistent with the expected values, and they were characterized by standard spectroscopic techniques (see Table 1), and by a X-ray diffraction study of complex **19** (see below).

(15) (a) Helling, J. F.; Hendrickson, W. A. *J. Organomet. Chem.* **1979**, *168*, 87. (b) Pauson, P. L.; Segal, J. A. *J. Chem. Soc., Dalton Trans.* **1975**, 1677.

(16) Manzur, C.; Fuentealba, M.; Millán, L.; Gajardo, F.; Carrillo, D.; Mata, J. A.; Sinbandhit, S.; Hamon, P.; Hamon, J.-R.; Kahlal, S.; Saillard, J.-Y. *New J. Chem.* **2002**, *26*, 213.

(17) Astruc, D.; Hamon, J.-R.; Roman, E.; Michaud, P. *J. Am. Chem. Soc.* **1981**, *103*, 7502.

(18) Trujillo, H.; Casado, C. M.; Astruc, D. *J. Chem. Soc., Chem. Commun.* **1995**, 7.

(19) Casado, C. M.; Wagner, T.; Astruc, D. *J. Organomet. Chem.* **1995**, *502*, 143.

(20) Trujillo, H.; Casado, C. M.; Ruiz, J.; Astruc, D. *J. Am. Chem. Soc.* **1999**, *121*, 5674.

(14) (a) López, C.; Bosque, R.; Solans, X.; Font-Bardia, M. *J. Organomet. Chem.* **1997**, *547*, 309. (b) López, C.; Granell, J. *J. Organomet. Chem.* **1998**, *555*, 211.

Both the N–H stretching vibration at $ca. 3350\text{ cm}^{-1}$ and the broad low-field signal at $ca. \delta 9.5\text{ ppm}$ vanished from the IR and ^1H NMR spectra, respectively. In the ^1H NMR spectra of compounds **18–20** (see Table 1) the aromatic protons of both coordinated and free C_6 -rings, the azomethine CH and Cp proton resonances, are observed in the same respective regions as those described above for the nonmethylated hydrazones **5–17**. Moreover, a new singlet assigned to the *N*-methyl proton resonance is now observed for each of the three derivatives **18–20**, in the 3.53–3.73 ppm region, in agreement with reported data for related compounds.^{15a,21}

Finally, the electronic absorption spectra of compounds **5–20** have been recorded in CH_2Cl_2 ($\mu = 8.90$) and DMSO ($\mu = 47.6$) (see Table 1). All complexes exhibit similar spectra, indicating similar structural features. The spectra of the complexes recorded in CH_2Cl_2 present, in the range 280–380 nm, a prominent complex band that consists of two or three overlapped absorption bands corresponding to intraligand CT excitations. Two of these bands observed in the range 310–380 nm are, for the majority of complexes, slightly red-shifted in DMSO. At longer wavelengths, $ca. 380\text{--}500\text{ nm}$, a very broad low-intensity MLCT band is also observed.^{6,24} The broadening of this low-energy band is probably the result of the overlap of broad d–d visible bands of the $[\text{CpFe}(\eta^6\text{-arene})]^+$ fragment.^{26,27} Solvatochromic effects can hint at the magnitude of the expected nonlinear optical properties, since they reflect the polarizability of a chromophore.^{27,28} However, in the present case, the magnitude of the solvatochromic effects could not be accurately determined due to the difficulty of assigning with sufficient accuracy their λ_{max} values.

2. Crystal Structures. The molecular structures of the cationic organometallic moieties, $[\text{CpFe}(\eta^6\text{-C}_6\text{H}_5\text{-NHN}=\text{CH}-\text{C}_6\text{H}_4\text{-}i>p\text{-Me})]^+$ (**6**⁺) and $[\text{CpFe}(\eta^6\text{-C}_6\text{H}_5\text{-N(Me)N}=\text{CH}-\text{C}_6\text{H}_4\text{-}i>p\text{-OMe})]^+$ (**19**⁺), along with the atom labeling scheme are presented in Figures 1 and 2, respectively. Key bond lengths and angles for **6**⁺ and **19**⁺ are listed in Table 3, and details of data collection and refinement are summarized in Table 2. High anisotropic thermal motion and/or disorder was observed for the carbon atoms of the Cp ligand in **19**⁺ (Figure 2), a phenomenon frequently encountered in such mixed-sandwich derivatives.^{12,16,29,30} The observed orientation is presumably due to partial rotation of the

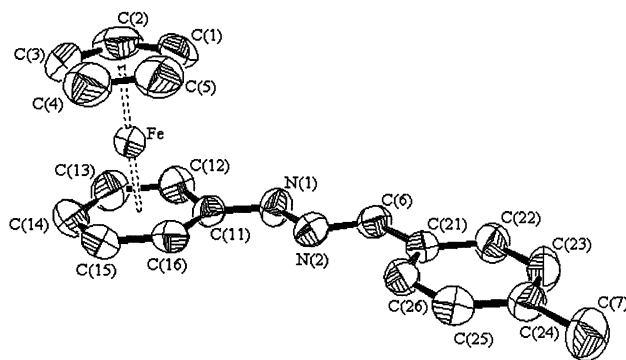


Figure 1. ORTEP view of cation $[\text{CpFe}(\eta^6\text{-C}_6\text{H}_5\text{-NHN}=\text{CH}-\text{C}_6\text{H}_4\text{-}i>p\text{-Me})]^+$ (**6**⁺) with the atom-labeling scheme. Hydrogen atoms and counteranion PF_6^- have been omitted for clarity. Displacement ellipsoids are at the 50% probability level.

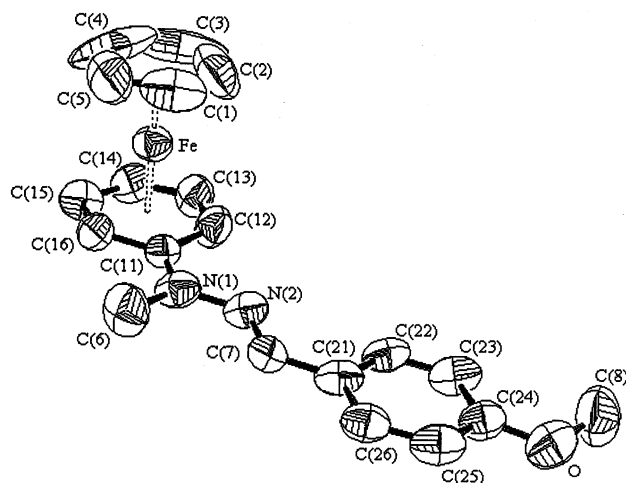


Figure 2. ORTEP view of cation $[\text{CpFe}(\eta^6\text{-C}_6\text{H}_5\text{-N(Me)N}=\text{CH}-\text{C}_6\text{H}_4\text{-}i>p\text{-OMe})]^+$ (**19**⁺) with the atom-labeling scheme. Hydrogen atoms and counteranion PF_6^- have been omitted for clarity. Displacement ellipsoids are at the 50% probability level.

C_5 ring about the Fe–Cp centroid axis. Inspection of the bond distances and angles between the two rings (see Table 3) clearly indicates a $\eta^5\text{-Fe}-\eta^6$ coordination mode for both compounds.^{31–33} More interestingly, in view of their solid-state structures, the phenyl rings of **6**⁺ and **19**⁺ show good coplanarity (dihedral angles between two phenyl rings are 4.9° and 6.2°, respectively), which is important for an efficient π -electron delocalization along the entire backbone and thus might ensure a large molecular nonlinearity in the crystalline solid.^{7c} This contrasts with greater rotations of the bromophenyl ring by $ca. 26^\circ$ ³³ and of the *N*-methylpyrid-4-yl group by 43.2°⁶ out of the coordinated phenyl ring plane in

(21) Lee, C. C.; Gill, U. S.; Sutherland, R. G. *J. Organomet. Chem.* **1981**, *206*, 89.

(22) Michaud, P.; Astruc, D. *J. Chem. Soc., Chem. Commun.* **1982**, 416.

(23) Moinet, C.; Raoult, E. *J. Organomet. Chem.* **1982**, *231*, 245.

(24) Le Beuze, A.; Lissilour, R.; Weber, J. *Organometallics* **1993**, *12*, 47.

(25) Hamon, J.-R.; Astruc, D.; Michaud, P. *J. Am. Chem. Soc.* **1981**, *103*, 758.

(26) Morrison, W. H.; Ho, E. Y.; Hendrickson, D. N. *Inorg. Chem.* **1975**, *14*, 500.

(27) Wong, H.; Meyer-Friedrichsen, T.; Farrell, T.; Mecker, C.; Heck, J. *Eur. J. Inorg. Chem.* **2000**, 631.

(28) (a) Paley, M. S.; Harris, J. M.; Looser, H.; Baumert, J. C.; Bjorklund, G. D.; Jundt, D.; Twieg, R. J. *J. Org. Chem.* **1989**, *54*, 3774. (b) McRae, E. G. *J. Phys. Chem.* **1957**, *61*, 562.

(29) (a) Marcen, S.; Jiménez, M. V.; Dobrinovich, I. T.; Lahoz, F. J.; Oro, L. A.; Ruiz, J.; Astruc, D. *Organometallics* **2002**, *21*, 326. (b) Ishii, Y.; Kawaguchi, M.; Ishino, Y.; Aoki, T.; Hidai, M. *Organometallics* **1994**, *13*, 5062. (c) Subramanian, S.; Wang, L.; Zaworotko, M. J. *Organometallics* **1993**, *12*, 310. (d) Fillaut, J.-L.; Boese, R.; Astruc, D. *Synlett* **1992**, 55. (e) Abboud, K. A.; Simonsen, S. H.; Pioroko, A.; Sutherland, R. G. *Acta Crystallogr.* **1991**, *C47*, 860.

(30) Manzur, C.; Fuentealba, M.; Carrillo, D.; Boys, D.; Hamon, J.-R. *Bol. Soc. Chil. Quim.* **2001**, *46*, 409.

(31) For examples of X-ray crystal structures of $[\text{CpFe}(\eta^6\text{-arene})]^+$ complexes, see: (a) Hamon, J.-R.; Saillard, J.-Y.; Le Beuze, A.; McGlinchey, M. J.; Astruc, D. *J. Am. Chem. Soc.* **1982**, *104*, 7549. (b) See also refs 6, 12, 29, and 33.

(32) For a reference gathering a large number of interatomic and metal–ligand distances obtained from the Cambridge Crystallographic Data Base Centre, see: Orpen, A. G.; Brammer, L.; Allen, F. H.; Kennard, D.; Watson, D. G.; Taylor, R. *J. Chem. Soc., Dalton Trans.* **1989**, S1. More than 50 X-ray crystal structures of $[\text{CpFe}(\eta^6\text{-arene})]^+$ derivatives can be found in this database system.

(33) Dyson, P. J.; Grossel, M. C.; Shrinivasan, M.; Vine, T.; Welton, T.; Williams, D. J.; White, A. J. P.; Zigras, T. *J. Chem. Soc., Dalton Trans.* **1997**, 3465.

Table 3. Selected Bond Distances (Å) and Angles (deg) of Cations 6⁺ and 19⁺^a

6 ⁺		19 ⁺	
Distances			
Fe–C(11)	2.174(3)	Fe–C(11)	2.197(5)
Fe–C(12–16) ^b	2.081	Fe–C(12–16) ^b	2.083
C(11)–N(1)	1.366(4)	C(11)–N(1)	1.383(6)
N(1)–N(2)	1.373(3)	N(1)–N(2)	1.374(5)
		N(1)–C(6)	1.465(5)
N(2)–C(6)	1.270(4)	N(2)–C(7)	1.275(6)
C(6)–C(21)	1.464(4)	C(7)–C(21)	1.440(7)
Fe–Cp _{CNT}	1.666	Fe–Cp _{CNT}	1.649
Fe–Ph _{CNT}	1.560	Fe–Ph _{CNT}	1.567
Angles			
C(11)–N(1)–N(2)	119.7(3)	C(11)–N(1)–N(2)	113.9(5)
N(1)–N(2)–C(6)	116.0(3)	N(1)–N(2)–C(7)	119.5(5)
N(2)–C(6)–C(21)	121.6(3)	N(2)–C(7)–C(21)	121.5(6)
		C(11)–N(1)–C(6)	123.9(5)
		C(6)–N(1)–N(2)	122.2(5)
Cp _{CNT} –Fe–Ph _{CNT}	178.3	Cp _{CNT} –Fe–Ph _{CNT}	177.9

^a Abbreviations: Cp = C₅H₅, Ph = C₆H₅; CNT = centroid.

^b Average bond distances.

[CpFe(η⁶-C₆H₅-C₆H₄-*p*-Br)]⁺ and [CpFe(η⁶-C₆H₅-N=C₅H₄NMe)]⁺, respectively.

A perusal of the molecular parameters of 6⁺ and 19⁺ reveals other interesting structural features. The Fe–C(11) bond lengths, 2.174(3) and 2.197(5) Å, respectively, are ca. 0.093 and 0.114 Å longer than the mean of the other Fe–C (C₆ ring) bond distances, and the C(11)–N(1) bond lengths of 1.366(4) Å for 6⁺ and of 1.383(6) Å for 19⁺ are at halfway of a single and double carbon nitrogen bond.³² The structural data reveal also a partial delocalization of the electron lone pair of the N(1) atom toward the cationic organometallic fragment, which involves its partial depyramidalization. This is clearly evidenced by the bond angles about the N(1) atom for 19⁺ (see Table 3). The sum of these bond angles is 360°, which indicates that the C(11), C(12), and N(2) atoms are coplanar with the sp²-hybridized N(1) atom. Moreover, the coordinated C₆-rings are folded up along the C(12)–C(16) axis with a dihedral angle of 6.2° in compound 6⁺ and 7.4° in compound 19⁺. These observations lead us to attribute a partial positive charge on the N(1) atom (iminium resonant form) and, consequently, a slight cyclohexadienyl character of the arene ring with a partial negative charge. These findings are in accord with previous structural data^{6,12,16,29b,30,34} and theoretical work,³⁵ clearly indicating that aminoarenes π-coordinated to 12-electron organometallic moieties adopt the general pattern consisting of an iminium-cyclohexadienyl character with a small folding angle (<10°) and a partial multiple-bond character for the C–N linkage.

3. Electrochemistry. As stated in the Introduction, the [CpFe(η⁶-arene)]⁺ complexes are known for their interesting redox behavior.^{27,36} Thus, it is of interest to examine the electronic influence of the *para*-donating R' substituents through the hydrazone skeleton and of the methylation of the benzylic nitrogen atom, using electrochemistry. In particular, one can scrutinize these

Table 4. Cyclic Voltammetry Data^a

compound	DMF		MeCN	
	E _{pc} (V) ^b	E _{pa} (V) ^c	E _{pc} (V) ^b	E _{pa} (V) ^c
5	–1.87	1.04	–1.42	1.44
6	–1.91	0.98; 1.31	–1.43	1.48
7	–1.93	0.94; 1.26	–1.74	1.26
8	–1.95	0.70	–1.92	0.73; 1.01
11	–1.98	0.66; 0.90	–1.80	0.69; 1.20
14	–1.97	0.70	–1.80	0.72; 1.19
17	–1.92	0.75	–1.86	0.79; 1.12
18	–1.35	1.42	–1.38	1.46
19	–1.38	1.33	–1.42	1.36
20	–1.40	1.23	–1.47	0.79; 1.29
TADNPH ^d		1.14; 1.32		1.46

^a Recorded in the stated solvent at 298 K with a vitreous carbon working electrode, 0.1 M *n*-Bu₄⁺PF₆[–] as supporting electrolyte, scan rate 100 mV s^{–1}. All potentials are quoted vs Ag/AgCl. ^b Irreversible wave corresponding to the Fe(II)/Fe(I) couple. ^c Irreversible oxidation process(es) corresponding to the hydrazone moieties. ^d TADNPH = *p*-tolualdehyde 2,4-dinitrophenylhydrazone.³⁹

influences in terms of thermodynamics via the redox potentials and the stability of the odd redox state via the shapes of the cyclovoltammetry waves. For this aim three selected series were chosen: (i) [CpFe(η⁶-C₆H₅-NHN=CH–C₆H₄-*p*-R')]⁺PF₆[–] (R' = H, **5**; Me, **6**; MeO, **7**; NMe₂, **8**), (ii) [CpFe(η⁶-*o*-RC₆H₄NHN=CH–C₆H₄-*p*-NMe₂)]⁺PF₆[–] (R = Me, **11**; MeO, **14**; Cl, **17**), and (iii) [CpFe{η⁶-C₆H₅N(Me)N=CH–C₆H₄-*p*-R'}]⁺PF₆[–] (R' = Me, **18**; MeO, **19**; NMe₂, **20**). The values of the reduction and oxidation potentials are given in Table 4. Cyclic voltammetry studies were carried out at room temperature using a vitreous carbon working electrode in both DMF and acetonitrile containing 0.1 M *n*-Bu₄N⁺PF₆[–] as supporting electrolyte. The number of electrons transferred was estimated by comparison with that of the Cp₂Fe^{0/+} couple under the same experimental conditions.

In DMF, the one-electron irreversible cathodic process observed for all the compounds studied corresponds to the single-electron reduction of the d⁶ Fe(II), 18-electron complexes to the d⁷ Fe(I), 19-electron species.^{27,36} Surprisingly, the non *N*-methylated hydrazone derivatives **5–8**, **11**, **14**, and **17** exhibit reduction potentials ca. 0.6 V more cathodic (Figure 3a) than those of their *N*-methylated analogues **18–20** (Figure 3c and Table 4). This unexpected behavior can be understood if one considers that the acidic *N*-H protons of the hydrazones **5–8**, **11**, **14**, and **17** are deprotonated by DMF, a more basic solvent than acetonitrile (see below).³⁷ This *N*-H group is strongly activated by both the electron-withdrawing organometallic moiety and the –N=CH–(Ar)imine group. Indeed, when the cyclovoltammogram of a freshly generated solution of the neutral red intermediate resulting from the deprotonation of **7** (see Section 1 and the molecule in square brackets in Scheme 2) is recorded, the irreversible reduction wave is observed at –1.92 V (Figure 3b). After addition of iodomethane (step 2 in Scheme 2), the electrochemical solution lightened, and the cyclovoltammogram shows a new reduction wave at –1.39 V (Figure 3c), ascribed to the corresponding *N*-Me hydrazone **19**. Obviously, such a zwitterionic intermediate cannot be generated

(34) Saillard, J.-Y.; Grandjean, D.; Le Maux, P.; Jaouen, G. *Nouv. J. Chim.* **1981**, 5, 153.

(35) Ruiz, J.; Ogliaro, F.; Saillard, J.-Y.; Halet, J.-F.; Varret, F.; Astruc, D. *J. Am. Chem. Soc.* **1998**, 120, 11693.

(36) Astruc, D. In *Electron Transfer and Radical Reactions in Transition-Metal Chemistry*; VCH: New York, 1995; Chapter 2, pp 147–149.

(37) Benoit, R. L.; Louis, C. In *The Chemistry of Nonaqueous Solvents*; Lagowski, J. J., Ed.; Academic Press: New York, 1978; Vol. VA, Chapter 2.

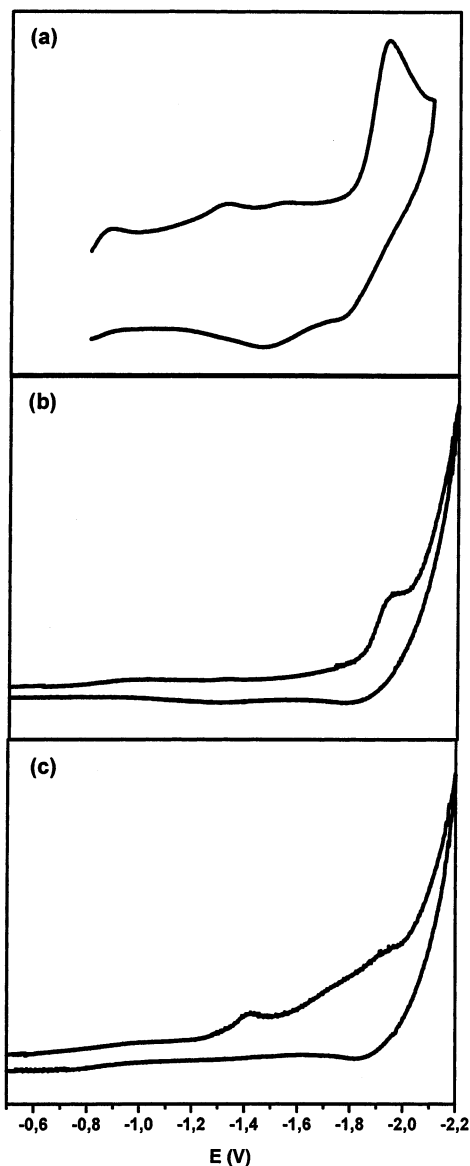


Figure 3. Cyclic voltammograms of (a) $[\text{CpFe}(\eta^6\text{-C}_6\text{H}_5\text{-NHN=CH-C}_6\text{H}_4\text{-}p\text{-OMe})]^+\text{PF}_6^-$ (**7**), (b) the zwitterionic intermediate generated by deprotonation of **7**, and (c) the *N*-methylated hydrazone **19** resulting from addition of MeI to the electrochemical solution, recorded in DMF/0.1 M *n*-Bu₄N⁺PF₆⁻ at $T = 20^\circ\text{C}$ and a voltage sweep rate $v = 0.1\text{ V s}^{-1}$.

from the *N*-Me hydrazones **18–20**. A larger cathodic shift, ca. 0.8 V, has also been found in DMSO by Astruc and co-workers, between the first reduction potential of the cationic complex $[\text{CpFe}(\eta^6\text{-C}_6\text{Me}_6)]^+$ and that of its neutral η^5 -benzyl counterpart $\text{CpFe}(\eta^5\text{-C}_6\text{Me}_5\text{CH}_2)$.²⁰ However, for the two series of compounds **5–8** and **18–20** the redox potentials become progressively more cathodic, from -1.87 to -1.95 V and from -1.35 to -1.40 V , respectively. This clearly indicates a significant electronic influence of the *para*-donating substituent on the iron center ($\text{H} < \text{Me} < \text{MeO} < \text{NMe}_2$), although a Hammett correlation could not be established. On the other hand, the influence of the *ortho*-R substituent at the coordinated phenyl ring ($\text{R} = \text{H, Me, MeO, Cl}$) of compounds **8, 11, 14**, and **17**, respectively, bearing the same *para*-NMe₂ donating group, is also noticeable.

Compound **17** is easier to reduce by 60 mV than its methylated counterpart **11**.

The cyclic voltammograms recorded in acetonitrile show also a mono-electronic irreversible reduction wave, which indicates that the 19-electron species is not stable for all the compounds studied (Table 4). In this solvent, the cyclic voltammograms are less well-behaved, except for the *N*-methylated hydrazones **18–20**, which exhibit behavior and trend similar to those observed in DMF. For the other complexes under investigation, the situation is more complicated. This could presumably be due to some intermolecular interactions of the benzylic *N*-H hydrogen with the basic groups (OMe, NMe₂) of neighboring molecules, or even with the PF₆⁻ ion.³⁸ The reduction potentials of compounds **5** and **6**, which do not bear *para*-donating substituents, are however in the expected range for such amino-substituted arene iron complexes,^{4,16} albeit slightly more negative than those of the *N*-methylated hydrazone counterparts (Table 4).

On the oxidation side, it is clear that in DMF the irreversible wave observed for complexes **5–8, 11, 14**, and **17** can be attributed to the oxidation of their respective neutral in situ generated zwitterions, by comparison of their oxidation potentials with that of the cationic *N*-methylated hydrazones **18–20** (Table 4). A more positive oxidation potential indicates that the hydrazone complex is more difficult to oxidize, i.e., less electron rich. In acetonitrile, it is interesting to note that compounds **5, 6**, and **18–20** are oxidized at the same potential as the organic hydrazone TADNPH,³⁹ the 2,4-(NO₂)₂C₆H₃- unit being recognized as electron withdrawing as the 12-electron cationic organometallic moiety $[\text{CpFe}^+]$.¹

Concluding Remarks

We report in this article an extension of the synthetic methodology, illustrating the scope and adaptability of the condensation reaction between π -coordinated hydrazines and organic¹² or organometallic^{16,30} carbonyl sources, leading to two new homogeneous series of monocationic organo-iron(II) benzaldehyde-hydrazones of general formula $[\text{CpFe}(\eta^6\text{-}o\text{-RC}_6\text{H}_4\text{NHN=CHC}_6\text{H}_4\text{-}p\text{-R}')^+\text{PF}_6^-$ ($\text{R} = \text{H, Me, MeO, Cl}$; $\text{R}' = \text{H, Me, MeO, NMe}_2$) and the *N*-methyl derivatives formulated as $[\text{CpFe}\{\eta^6\text{-C}_6\text{H}_5\text{N(Me)N=CHC}_6\text{H}_4\text{-}p\text{-R}'\}]^+\text{PF}_6^-$ ($\text{R}' = \text{Me, MeO, NMe}_2$). Those later compounds result from a benzylic *N*-H bond activation of the former hydrazone precursors and subsequent *N*-C bond formation of the deprotonated species with iodomethane. The zwitterionic or iminocyclohexadienyl intermediates have been clearly identified by their irreversible reduction waves at very low potentials close to -2 V in DMF, whereas those of the cationic *N*-methylated hydrazones **18–20** are anodically shifted by 0.6 V to the expected range at ca. -1.40 V .

All the organometallic hydrazones described in this work can be defined as type I non-rod-shaped dipolar chromophores.^{7a,b} The cationic mixed-sandwich $[\text{CpFe}(\eta^6\text{-}o\text{-RC}_6\text{H}_4\text{-})]^+$ acts as an electron acceptor and the

(38) Manzur, C.; Fuentealba, M.; Millan, L.; Gajardo, F.; Garland, M. T.; Baggio, R.; Mata, J. A.; Hamon, J.-R.; Carrillo, D. *J. Organomet. Chem.* **2002**, *660*, 71.

(39) Rappoport, Z. *Handbook of Tables for Organic Compounds Identification*, 3rd ed.; CRC Press: Cleveland, OH, 1967; p 148.

para-substituted free arene group $-\text{C}_6\text{H}_4\text{-}p\text{-R}'$ as an electron donor. Their mutual electronic influence is warranted by the hydrazone linking spacer $-\text{NH}-\text{N}=\text{CH}-$. The electronic cooperativity expresses itself through the electron-releasing effects of the *para*-R' substituent of the aldehyde fragment, $=\text{CH}-\text{C}_6\text{H}_4\text{-}p\text{-R}'$, on the observed reduction potentials. On the other hand, the favorable electronic structure resulting from the coplanarity of both coordinated and free phenyl rings of the hydrazone ligand allows the charge transfer process to extend from the donor to the acceptor termini, through the entire hydrazone skeleton. Work is now directed toward the isolation, full characterization, and functionalization with organic moieties and substrates of biological interest of the zwitterionic intermediate and to determine the potential optical properties of some selected species of the new dipolar organometallic hydrazone complexes reported in this paper.

Acknowledgment. We thank Prof. C. Moinet (Rennes) for helpful comments on electrochemistry, Drs. P. Jehan and P. Guénot (CRMPO, Rennes) for mass

spectrometry assistance, and M. Fuentealba (Valparaíso) for skillful experimental assistance. We greatly appreciate financial support for this work from the Fondo Nacional de Desarrollo Científico y Tecnológico, FONDECYT, Grant No. 1000281 (C.M.), the Programme International de Coopération Scientifique, CNRS-CONICYT, PICS No. 922, 2000-02, (C.M., D.C., J.-R.H.), and the Universidad Católica de Valparaíso, Chile. We also thank Fundación Andes for funding the purchase of the single-crystal diffractometer.

Supporting Information Available: Tables giving reaction stoichiometries and yields of organo-iron hydrazone complexes **1**–**4** with benzaldehydes (Table S1) and of the preparation reactions of the *N*-methylated hydrazones **18**–**20** (Table S2), and the melting points and analytical data for all the new compounds (Table S3); tables of crystal data, atomic coordinates, bond distances and angles, and anisotropic displacement parameters for complexes **6** and **19**. This material is available free of charge via the Internet at <http://pubs.acs.org>.

OM020672T